Ferromagnetism in Dilute Magnetic Semiconductors through Defect Engineering: Li-Doped ZnO

J. B. Yi,[1,*] C. C. Lim,[2] G. Z. Xing,[3] H. M. Fan,[1] L. H. Van,[4] S. L. Huang,[3] K. S. Yang,[2,5] X. L. Huang,[1] X. B. Qin,[6]
B. Y. Wang,[6] T. Wu,[3] L. Wang,[3] H. T. Zhang,[1] X. Y. Gao,[2] T. Liu,[2] A. T. S. Wee,[2] Y. P. Feng,[2,†] and J. Ding[1,‡]

[1]*Department of Materials Science and Engineering, National University of Singapore, 119260, Singapore*
[2]*Department of Physics, National University of Singapore, 2 Science Drive 3, 117542, Singapore*
[3]*School of Physical and Mathematical Sciences, Nanyang Technological University, 637371, Singapore*
[4]*Nanoscience and Nanotechnology Initiative, National University of Singapore, Singapore, 119260*
[5]*Department of Physics, Shandong University, Jinan, China*
[6]*Key Laboratory of Nuclear Analysis Techniques, Institute of High Energy Physics, Chinese Academy of Sciences,
Beijing 100049, China*

We demonstrate, both theoretically and experimentally, that cation vacancy can be the origin of ferromagnetism in intrinsic dilute magnetic semiconductors. The vacancies can be controlled to tune the ferromagnetism. Using Li-doped ZnO as an example, we found that while Li itself is nonmagnetic, it generates holes in ZnO, and its presence reduces the formation energy of Zn vacancy, and thereby stabilizes the zinc vacancy. Room temperature ferromagnetism with p type conduction was observed in pulsed laser deposited ZnO:Li films with certain doping concentration and oxygen partial pressure.

Because of potential applications in spintronics, the dilute magnetic semiconductor (DMS) has attracted much attention. The original idea of DMS was to dope magnetic elements such as Mn into a semiconductor host to make the semiconductor magnetic at room temperature [1,2]. Among the potential host materials for DMS, ZnO has been extensively studied since it was predicted to be a promising host material to achieve room temperature DMS [3]. Room temperature ferromagnetism (RTF) was indeed observed in ZnO-based DMS [4–8]. However, the origin of the observed ferromagnetism is unclear, and the existing theories [3,9] cannot satisfactorily explain the observed phenomena. Recently, RTF was observed in semiconductors or oxides doped with nonmagnetic elements [7] as well as undoped oxides such as ZnO, TiO_2, In_2O_3, and HfO_2 [10,11], and the ferromagnetic properties of these materials are strongly dependent on sample preparation. The correlation between ferromagnetism and sample preparation conditions suggests that defects may play an important role in the observed magnetic behaviors of these materials. Therefore, how to control and engineer defects becomes a very interesting and challenging issue. It would be very useful if defects in these materials can be manipulated to improve the properties of DMSs.

Theoretical studies have been carried out to investigate the mechanisms of ferromagnetism associated with defects. The results of first-principle calculations indicate that neutral oxygen vacancy in ZnO is nonmagnetic [12], but Zn vacancy does lead to magnetism [13,14]. We carried out first-principles calculations based on density functional theory (DFT), using the Vienna *ab initio* simulation package (VASP) [15] and confirmed that a neutral oxygen vacancy in ZnO is nonmagnetic, but each Zn vacancy carries a magnetic moment of $\sim 1.30 \mu_B$. However, the formation energy of neutral cation (Zn) vacancy in ZnO is very high. Even though charged state of Zn vacancies can easily form in n-type samples and under oxygen-rich condition, this is not the case in p-type samples and oxygen-poor conditions [16]. Furthermore, our investigation on magnetic property of the 2- charged state of Zn vacancies shows that it is nonmagnetic. Thus, undoped ZnO is nonmagnetic under the normal circumstances.

Cation vacancies introduce local magnetic moments as well as holes to the host semiconductor, and ferromagnetism in such a DMS can be mediated by holes. Recently, Peng *et al.* pointed out that a threshold hole concentration is necessary to induce RTF [17]. Therefore, to enhance ferromagnetism in ZnO, one way is to stabilize cation vacancies and introduce holes at the same time. This can be achieved by doping with proper elements. Lithium (Li) is an element that can be easily incorporated into ZnO, and it is often used to produce p-type ZnO [18,19]. Therefore, we focus on Li doping in ZnO in this study. We demonstrate that by doping with Li, RTF can be achieved in ZnO by the stabilization of cation vacancies. The mechanism of ferromagnetism is discussed.

The samples were fabricated by pulse laser deposition (PLD). The details for the sample preparation and film characterization can be found in the supplementary document [20]. X-ray diffraction (XRD) study shows that high quality epitaxial (002)-ZnO films were grown on the (001) quartz substrate. Using a properly aligned high-resolution XRD system, we examined the (002) and (100) peaks and derived the lattice parameters a, c and unit cell volume for the hexagonal wurtzite ZnO structure with various Li doping concentrations. As shown in Fig. 1(a), the doping of ZnO with Li was accompanied by a lattice expansion for Li concentration up to 4 at%, but further increase in Li
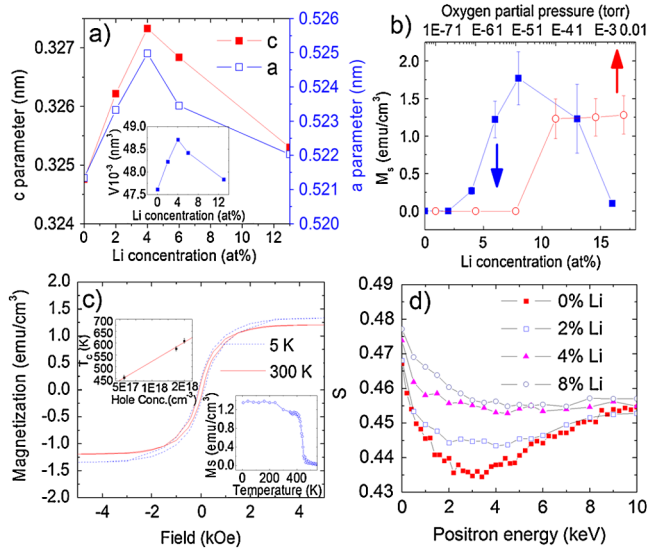
FIG. 1 (color online).   (a) Lattice parameters a and c of Li-doped ZnO as a function of Li doping concentration. The inset shows the dependence of the ZnO unit cell volume on Li doping concentration. (b) M_S dependence on Li doping concentration at $PO_2 = 10^{-4}$ torr (square) and on PO_2 for 6% Li-doped ZnO (circle), respectively. (c) Hysteresis loops of 6% Li-doped ZnO measured at 5 and 300 K, respectively. The insets show variations of magnetization with temperature (lower-right) and Curie temperature (T_C) with the corresponding hole concentration (upper-left). (d) The spectra of S parameter versus incident positron energy.

doping concentration beyond 4 at% resulted in a reduction of the unit cell volume. These results suggest that Li atoms prefer interstitial sites at low concentration, while additional Li atoms replace Zn sites when the Li doping concentration exceeds a certain threshold (3–4 at%). The result was confirmed by x-ray photoelectron spectroscopy. For the film with Li concentration of 4 at% and below, only a single peak at 53 eV was observed. At higher Li doping concentration, however, another prominent peak was observed at 55 eV, in addition to the one at 53 eV (Ref. [20], Fig. S3). It is known that the peak at 53 eV is associated with Li interstitial while that at the higher energy is an indication of formation of Li-O bond [19].

Transport measurement (Table I) shows that ZnO:Li deposited under a constant oxygen partial pressure (PO_2) of 10^{-4} torr behaved as an n-type semiconductor when Li doping concentration is low (0–4 at%). However, when Li doping concentration increased beyond 4 at%, the film switched to a p-type behavior, and it remained p-type until Li doping concentration reached 13 at%. The film with a doping concentration of 16 at% became amorphous and insulating. The transport property is also dependent on PO_2 (Table II). At a fixed Li concentration (6 at%), the film was n-type at low PO_2, but changed to p-type if PO_2 was increased to above 10^{-5} torr. Figure 1(b) shows the dependence of saturation magnetization (M_S) on Li doping concentration. RTF starts to appear at 4 at% and reaches a

maximum at 8 at% (i.e., when the sample has p-type behavior). RTF eventually disappears at 16 at%, which is insulating. We also examined the dependence of M_S of the ZnO:Li films on PO_2 under a constant Li concentration of 6 at% [Fig. 1(b)]. The film became ferromagnetic when PO_2 was $>10^{-4}$ torr. Further increase in PO_2 (e.g., 10^{-3} torr) resulted in a slight increase in M_S of the film, and M_S did not show any significant change up to the maximum PO_2 achievable in our PLD system (5×10^{-3} torr). Hysteresis loops obtained at 5 and 300 K are shown in Fig. 1(c). The coercivity of the film at 300 K ($H_C = 80$ Oe) confirms the RTF. Curie temperature (T_C) of ZnO:Li was measured using SQUID oven, and are given in Table I and II. As an example, we show in the lower-right inset of Fig. 1(c) the M_S dependence on temperature for ZnO film doped with 6% Li. The T_C of the film is approximately 454 K. The 8% Li-doped film shows the highest T_C. Variation of T_C with PO_2 is similar to that of M_S of the 6% Li-doped ZnO with PO_2, as shown in Fig. 1(b) (Ref. [20], Fig. S7). T_C of both samples also increase with PO_2, as seen in Table II. From the correlation between RTF and carrier types/T_C of the samples, we can conclude that ferromagnetism in Li-doped ZnO is accompanied by a p-type semiconductivity, and M_S/T_C increases monotonically with increasing hole concentration. The upper-left inset of Fig. 1(c) shows T_C of the 6% Li-doped ZnO deposited with different PO_2 as a function of hole concentration as shown in Table II. The data points can be well fitted with $T_C \propto P^{1/3}$. Similarly, T_C of ZnO:Li with Li doping concentrations of 4–13 at% versus corresponding

TABLE I.   Transport and magnetic properties of ZnO:Li with different Li doping concentrations (PO_2: 10^{-4} torr).

Li (at%)	Resistivity ($\Omega \cdot cm$)	Mobility ($cm^2/V \cdot s$)	Carrier Type Conc. (cm^{-3})	T_C (K)
0	1.7	28.3	-1.3×10^{17} (n)	$\cdots$
0.4 ± 0.1	2.6×10^{-2}	57.2	-4.2×10^{18} (n)	$\cdots$
2 ± 0.3	0.1	19.5	-3.2×10^{18} (n)	$\cdots$
4 ± 0.4	0.9	16.9	4.1×10^{17} (p)	433
6 ± 0.6	2.7	4.5	5.1×10^{17} (p)	454
8 ± 0.8	0.4	2.9	5.4×10^{18} (p)	525
13 ± 1.3	3.1	4.2	4.8×10^{17} (p)	439
16 ± 1.6	insulating	$\cdots$	$\cdots$	$\cdots$

TABLE II.   Transport and magnetic properties of 6%Li-doped ZnO under various oxygen partial pressures.

PO_2 (torr)	Resistivity ($\Omega \cdot cm$)	Mobility ($cm^2/V \cdot s$)	Carrier Type Conc. (cm^{-3})	T_C (K)
1×10^{-6}	9.7×10^{-3}	28.0	-2.3×10^{19} (n)	$\cdots$
1×10^{-5}	1.4×10^{-2}	59.5	-7.5×10^{18} (n)	$\cdots$
1×10^{-4}	2.7	4.5	5.1×10^{17} (p)	454
1×10^{-3}	2.1	1.7	1.8×10^{18} (p)	576
5×10^{-3}	1.9	1.6	2.1×10^{18} (p)	609

hole concentration, as shown in Table I, can also well be fitted with $T_C \propto P^{1/3}$ (Ref. [20], Fig. S9), confirming that the ferromagnetism in Li-doped ZnO is hole-mediated [3,21]. It is to note that ZnO:Li which are ferromagnetic showed magnetoresistance at both 5 and 300 K. However, anomalous Hall effect (AHE) could only be observed at low temperature.

The variation of M_S with PO$_2$ indicates that ferromagnetism in ZnO:Li may be associated with Zn vacancies, as a high PO$_2$ favors the formation of Zn vacancies and suppresses the formation of oxygen vacancies [22]. To understand the mechanism of RTF in Li-doped ZnO, we carried out first-principles calculations based on DFT. The calculations were performed using the VASP code, with the projector augmented wave (PAW) potential for electron-ion interaction and generalized gradient approximation (GGA-PBE) for electron exchange and correlation. A supercell consisting of $3 \times 3 \times 2$ unit cells of ZnO was used for defect calculations. Using a cutoff energy of 450 eV and a k-point grid of $2 \times 2 \times 3$, energy calculation was converged to within 10^{-4} eV while the force on an atom was less than 0.02 eV/Å. Results of our calculations show that Li interstitial (Li$_I$) results in an n-type semiconductor while Li substitutional doping at the cation site (Li$_{Zn}$) leads to p-type semiconductor [Fig. 2(a)], i.e., Li$_I$ contributes electrons while Li$_{Zn}$ generates holes in ZnO. Furthermore, our results show that Li dopant, in either interstitial form or substitutional form, does not result in a magnetic moment directly. Therefore, if Li contributes to ferromagnetism in ZnO, it can only do so by stabilizing other defects which are magnetic. Earlier works [13,14], as well as our calculations, show that Zn vacancy in ZnO (V$_{Zn}$) prefers a spin polarized state, and each V$_{Zn}$ carries a magnetic moment of $1.33\mu_B$ [see DOS in Fig. 2(a)]. Our work is thus focused on lowering the formation energy of V$_{Zn}$ and the role played by Li dopants.

The calculated defect formation energies of various types of concerned defects are shown in Fig. 2(b) as a function of oxygen chemical potential which is measured
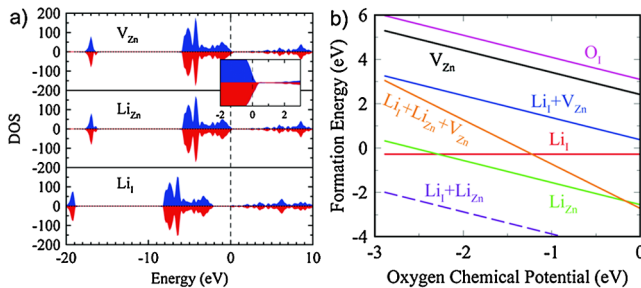
FIG. 2 (color online). (a) Total DOS of ZnO with a Li dopant at interstitial site (bottom panel), a substitutional Li dopant at the Zn site (middle panel), and a Zn vacancy (top panel), respectively. The inset shows the details around the Fermi level of V$_{Zn}$ which is indicated by the vertical dashed line. (b) Formation energies of various concerned defects are shown as functions of oxygen chemical potential.

relative to the energy of an oxygen atom in an oxygen molecule. The chemical potential of Li is taken as the energy of bulk metallic Li in bcc form which is the upper bound of Li chemical potential. The lower bound of the Li chemical potential corresponds to that in lithium oxide, which may not be much lower than the above value since lithium oxide is not a very stable compound. As seen in Fig. 2(b), Zn vacancy has a very high formation energy for the entire range of oxygen chemical potential which indicates that Zn vacancy is very difficult to form under the normal circumstances. Pure ZnO samples deposited at PO$_2$ as high as 5×10^{-3} torr do not show any ferromagnetism. However, presence of a Li interstitial in the proximity of V$_{Zn}$ lowers the formation energy of Zn vacancy significantly. The formation energy of a defect complex consisting of a Li interstitial and a Zn vacancy is more than 2 eV lower than the formation energy of a single Zn vacancy. Furthermore, if a Zn vacancy is accompanied by a Li interstitial and an additional substitutional defect Li$_{Zn}$, its formation energy can be further lowered. The formation energy of this defect complex becomes negative at high chemical potential. Therefore, results of our first-principles calculations suggest that Li doping contributes to ferromagnetism in ZnO by lowering the formation energy of Zn vacancy and thereby stabilizing Zn vacancy from which the magnetic moments originate.

As a matter of fact, Fig. 2(b) shows that except for the Li$_I$ + Li$_{Zn}$ defect complex which is discussed below, the most stable defect formed at low oxygen chemical potential is Li interstitial. As the oxygen chemical potential increases, Li$_{Zn}$ becomes more stable. With further increase in oxygen chemical potential, the defect complex Li$_I$ + Li$_{Zn}$ + V$_{Zn}$ becomes the most stable defect type. We also considered other types of simple and complex defects and found that their formation energies are higher, except for the Li$_I$ + Li$_{Zn}$ defect complex which is exceptionally stable throughout the entire range of oxygen chemical potential. This is due to significant local structural relaxation and the similarity between Li$_I$ + Li$_{Zn}$ and replacement of one Zn atom by two Li atoms which preserves the charge neutrality. However, at low Li concentration, the probability for Li$_I$ and Li$_{Zn}$ to be in close proximity to form the defect complex is low and the dominant defect forms should be Li interstitials and substitutional defects, and even if they encounter each other and form the defect complex, they do not result in magnetism. It is noted that at high oxygen chemical potential, there is also a possibility of forming oxygen interstitial (O$_I$). However, our calculations show that the formation energy of O$_I$ is much higher [Fig. 2(b)] and O$_I$ should not make any significant contribution.

Based on the calculated formation energies and magnetic properties of various types of defects, the dependence of magnetization of ZnO:Li on PO$_2$ can be easily understood. At low oxygen partial pressure or low chemical potential, Li dopant will be mainly in interstitial form. At a moderate PO$_2$ or chemical potential, Li$_{Zn}$ becomes the

dominant defect form in the sample. Our spin polarized DFT calculations indicate that Li in both interstitial form and substitutional form does not result in magnetism. Therefore, Li-doped ZnO is nonmagnetic at low PO_2. At high PO_2 or chemical potential, the defect complex $Li_I + Li_{Zn} + V_{Zn}$ starts to form. Based on results of our calculation and earlier work, Zn vacancy results in a magnetic moment associated with the defect. Here, each $Li_I + Li_{Zn} + V_{Zn}$ defect complex was found to contribute a magnetic moment of $1.1\mu_B$ which mainly comes from the Zn vacancy. These local magnetic moments can be coupled ferromagnetically by holes introduced by Zn vacancies and Li substitutional doping, resulting in a ferromagnetic ZnO at room temperature.

Based on this mechanism, we can also understand the evolution of electronic and magnetic properties of ZnO:Li. At low Li doping concentration and moderate PO_2, the formation energy of Li interstitial is relatively low. We can expect Li mainly appears as interstitial in ZnO. The Li interstitials bring in excess electrons to ZnO, and the sample is therefore n-type. The experimentally observed lattice expansion also confirms presence of Li interstitials. As Li increases, the interstitial sites would be saturated or the remaining interstitial sites become increasingly less energetically favorable. Li then starts to occupy the substitutional sites which leads to the shrink of lattice because of the smaller size of Li atom compared to Zn. Since Li_{Zn} generates holes, with further increase in Li concentration, the hole concentration increases. When Li concentration reaches a certain level, holes eventually dominate over electrons in the system, and the system begins to show p-type behavior. However, the system remains nonmagnetic because both Li interstitial and substitutional defects are nonmagnetic. With further increase in Li doping concentration, Li may form more complicated defect complex such as $Li_I + Li_{Zn} + V_{Zn}$ which lowers the formation energy of Zn vacancy significantly. Zn vacancies introduce magnetic moments as well as additional holes. Ferromagnetic coupling of these local moments could be mediated by the high concentration of holes introduced by Li_{Zn} and V_{Zn}, resulting in the observed RTF.

In this work, positron annihilation spectroscopy (PAS) was carried out to detect cation vacancies [23]. The relationship between the S values and positrons energy for the films is shown in Fig. 1(d). The increase in the S values with increasing dopant concentrations indicates that the doping of Li introduces more Zn vacancy-type defects. On the other hand, the continuous increase in S with Li concentration also excludes the precipitates in Li-doped ZnO. Presence of large amount of Zn vacancies in ferromagnetic films was also confirmed by photoluminescent (PL) measurement with a PL peak at 2.35 eV for 6% Li-doped ZnO [24].

In conclusion, using Li-doped ZnO as an example, we have demonstrated that cation vacancies can lead to ferromagnetism in DMS or oxides. However, such vacancies are normally very difficult to form, compared to anion vacancies, for example. Doping with appropriate elements can stabilize the cation vacancies and produce holes at the same time, which are required to mediate the ferromagnetism. Li appears in interstitial form in ZnO at low concentration or low oxygen chemical potential, and substitutes Zn at moderate concentrations, but neither results in local magnetic moments. At sufficiently high concentration, the Li interstitial and substitutional defects form a stable defect complex which helps to lower the formation energy of Zn vacancy. The observed ferromagnetism in ZnO:Li at room temperature is attributed to magnetic moments of cation vacancies mediated by holes introduced by Li_{Zn} and V_{Zn}. We expect this technique of engineering defects can be used to tune the magnetic properties of other materials.

*mseyj@nus.edu.sg
†phyfyp@nus.edu.sg
‡msedingj@nus.edu.sg

[1] H. Ohno *et al.*, Nature (London) **408**, 944 (2000).
[2] A. Oiwa *et al.*, Phys. Rev. Lett. **88**, 137202 (2002).
[3] T. Dietl *et al.*, Science **287**, 1019 (2000).
[4] K. A. Griffin *et al.*, Phys. Rev. Lett. **94**, 157204 (2005).
[5] S. B. Ogale *et al.*, Phys. Rev. Lett. **91**, 077205 (2003).
[6] J. B. Yi *et al.*, Adv. Mater. **20**, 1170 (2008).
[7] H. Pan *et al.*, Phys. Rev. Lett. **99**, 127201 (2007).
[8] S. Chawla *et al.*, Phys. Rev. B **79**, 125204 (2009).
[9] J. M. D. Coey *et al.*, Nature Mater. **4**, 173 (2005).
[10] N. H. Hong *et al.*, Phys. Rev. B **73**, 132404 (2006).
[11] M. Venkatesan *et al.*, Nature (London) **430**, 630 (2004).
[12] C. H. Patterson, Phys. Rev. B **74**, 144432 (2006).
[13] D. Galland and A. Herve, Phys. Lett. A **33**, 1 (1970).
[14] Q. Wang *et al.*, Phys. Rev. B **77**, 205411 (2008).
[15] G. Kresse and J. Hafner, Phys. Rev. B **47**, 558 (1993).
[16] A. Janotti and C. G. Van de Walle, Phys. Rev. B **76**, 165202 (2007).
[17] H. W. Peng *et al.*, Phys. Rev. Lett. **102**, 017201 (2009).
[18] B. Xiao *et al.*, Appl. Surf. Sci. **253**, 895 (2006).
[19] J. G. Lu *et al.*, Appl. Phys. Lett. **89**, 112113 (2006).
[20] See supplementary information at http://link.aps.org/supplemental/10.1103/PhysRevLett.104.137201 for additional details.
[21] T. Dietl *et al.*, Phys. Rev. B **63**, 195205 (2001).
[22] A. F. Kohan *et al.*, Phys. Rev. B **61**, 15019 (2000).
[23] F. A. Selim *et al.*, Phys. Rev. Lett. **99**, 085502 (2007).
[24] T. Moe Børseth *et al.*, Appl. Phys. Lett. **89**, 262112 (2006).